Experimental and numerical calibration in a critical flow venturi of close to sonic flow

Calibración experimental y numérica de flujo cercano al sónico en un Venturi de flujo critico

RIVERA-LÓEPZ, Jesús Eduardo*†, ARCINIEGA-MARTÍNEZ, José Luis, LÓPEZ-AGUADO-MONTES, José Luis and GUTIERREZ-PAREDES, Guadalupe Juliana

Instituto Politécnico Nacional, Escuela Superior de Ingeniería Mecánica y Eléctrica Unidad Azcapotzalco, México.

ID 1st Author: *Jesús Eduardo, Rivera-López* / **ORC ID:** 0000-0003-3988-9305, **CVU CONAHCYT ID:** 161653

ID 1st Co-author: *José Luis, Arciniega-Martínez* / **ORC ID:** 0000-0003-4996-8146, **CVU CONAHCYT ID:** 161637

ID 2nd Co-author: *José Luis, López-Aguado-Montes* / **ORC ID:** 0009-0009-6322-4937, **CVU CONAHCYT ID:** 229257

ID 3rd Co-author: *Guadalupe Juliana, Gutierrez-Paredes* / **ORC ID:** 0000-0003-2918-7377, **CVU CONAHCYT ID:** 122745

Abstract

This work introduces a new study in discharge coefficient performance in *CFV* when the throat flow is close to sonic regime $Ma \approx 1$ and the throat strangulation is not fully developed. Thus, two *CFV* of 0,56 and 2,24 mm diameter were experimentally calibrated by applying the volume averaging method; experimental calibration allowed to estimate C_d and measure uncertainty, for 2,24 mm diameter C_d is 7,34% higher than for 0,56 mm diameter when Ma global is 7,30 % higher. Based on experimental calibration results and *CFV* geometries, numerical experiments were realized to explain how $Ma \approx 1$ flow deviates C_d from the theoretical value, concluding compressibility affects thickness scrolling relation since it is 35,92% smaller for 2,24 mm diameter than 0,56 mm, giving a better approximation for C_d to the theoretical value for this throat diameter. Finally, numerical C_d models were obtained to evaluate the deviation these flow conditions produce in respect of empirical and numerical models, finding the numerical model's maximum error is 6,68% and the empirical model's maximum error is 1,64% under identical stagnation conditions.

Critical flow venturi, Sonic flow, Experimental calibration

Resumen

Este trabajo presenta un nuevo estudio del comportamiento del coeficiente de descarga en *CFV* cuando el flujo en la garganta está próximo al régimen sónico $Ma \approx 1$ y la estrangulación en la garganta no se alcanzó por completo. Para ello, se calibro experimentalmente dos *CFV* de 0,56 y 2,24 mm de diámetro de garganta por el método de acumulación de volumen; con la calibración experimental se estimó el C_d y la incertidumbre de la medición, encontrando que el diámetro de garganta de 2,24 mm es 7,34 % más alto respecto a 0,56 mm cuando el Ma global es 7,30 % más elevado. Con los resultados de la calibración experimental y con la geometría de los *CFV* se realizaron experimentos numéricos con el objetico de explicar como el flujo $Ma \approx 1$ desvía al C_d del valor teórico, encontrando que la compresibilidad afecta la relación del espesor de desplazamiento δ^*/d, ya que es 35,92 % más pequeño para el diámetro de 2,24 mm en comparación de 0,56 mm, provocando que el C_d tenga una mejor aproximación al valor teórico para este diámetro de garganta. Finalmente se obtuvieron modelos numéricos del C_d para cada diámetro de garganta con el objetivo de tener una forma de evaluar la desviación que produce estas condiciones de flujo con respecto a modelos empíricos y numéricos, encontrando que los modelos numéricos tienen un error máximo de 6,68 % y los modelos empíricos el error máximo es de 1,64 % en condiciones de estancamiento iguales.

Venturi de flujo crítico, Flujo sónico, Calibración experimental

* Correspondence of the Author (E-mail: jriveral@ipn.mx)
† Researcher contributing as first author.

Introduction

In vapor generation in the electrical industry, natural gas plays an important role in the replacement of coal and fuel oil, since it is a cheaper fuel and has more calorific power, talking about energy supplied. It implies vapor generation cost reduces to 80% by using natural gas. Traditionally, subsonic devices have been used ($Ma \leq 0,3$) to measure natural gas flow. However, these low uncertainty devices 0,3 to 3,0% [10] lose millions of dollars because of measuring uncertainty. Consequently, metrology laboratories and research centers have developed investigations on critical flow measure elements ($Ma = 1$). These measure devices are known as Critical Flow Venturi (*CFV*), where the uncertainty range for these devices goes between 0,03 and 0,3 [10]. This inherent property makes them a superior measure device compared to subsonic measure devices. The *CFV*s are calibrated by using air and applied in natural gas measure, their performance range oscillates from 10 to 300 m^3 / h, with pressures to 700 kPa [14]. Measure quality depends directly on the discharge coefficient magnitude, C_d, which comprises every irreversibility on gas flow measure and *CFV* geometry. Some irreversibilities causing derivation of C_d from the theoretical value are, for example, viscous diffusivity, compressibility effects, thermal boundary layer [12], hydrodynamics' boundary layer thickness, entrance geometry, rugosity, humidity, chemical gas composition, etc. The research spectrum to understand and improve deviation mechanisms from theoretical value is extremely wide, for example, Chunhui [4] focused his study on how throat diameter affects flow characteristics, he measured a discharge coefficient of 21 super *CFV* in a flow range from 2,39 X 10^4 to 2,8 X 10^6 *Re*, obtaining C_d can variate to 2,3% for identical throat diameters under different stagnation pressures, concluding to have precise C_d values, similar calibration stagnation pressures are required. Jae Hyung Kim [11] realized another computational study focused on geometry effects on C_d, where he variated the diffuser angle from 2 to 8° and throat diameter from 0,2 to 5 mm, where it was found for throat diameters less than 2 mm the diffusor angle affects C_d considerably and it would be affected the most as less as the throat diameter is, this because of sonics line ubication, which is more significant for smaller diameters.

Junji Nagao [13] realized numerical research about state effects equations on C_d by using H_2 as a working fluid, where Redliche-Kwon and Lee-Kesler equations have good behavior on C_d at high *Re*, but also C_d decreases while *Re* increases when $1,0$ X $10^5 < Re < 2,8$ X 10^6. On the other hand, Ishibashi [15] developed a theoretical model from Hall's equation in the viscous zone and Geropp's equation about the boundary layer, he verified his model by the calibration of 25 super *CFV*s, resulting for *Re* > 8 X 10^4 theoretical and experimental coefficients' difference is 0,04%. Aaron [2] used dimensional metrology to measure curvature and throat diameter for nine *CFVs*, by throat curvature and Stratford-Kliegel and Gerrop-Kliegel theoretical C_d models he determined a C_d theoretical model for laminar, transition, and turbulent flow, in a range from 7,2 X 10^4 to 2,5 X 10^6 *Re*, where diameter and throat curvature corrections realized to theoretical models show good results since deviation respect to experimental coefficient is less than 0,017 and 0,07% for turbulent and laminar flow respectively. Ishibashi [7] in transition flow, studied C_d dependence on concerning curvature, entrance diameter, and diffusor longitude, to do this, he designed ten super *CFV*s, finding an empirical C_d equation that involves the whole ISO 9300 flow regimen. The experimental results were compared with the Stratford equation and Hall-Geropp combined equation, concluding Geropp's equation is precise enough, which does not happen with Hall and Stratford's when the entrance curvature is small. Mickan [3] presents the C_d numerical calculus based on laminar and turbulent boundary layer integral methods, the results were compared with experimental measures on laminar and turbulent regimes, verifying good quality in numerical results. Critical and sonic flow in Venturi nozzles gas flow measure is the throat flow necessary condition for the approximation of discharge coefficient to unity, hence sonic nozzles work in the turbulent and sonic range. For this reason, investigations are focused on solving the inherent problems at this flow condition, that's why the present work objective is to study the compressibility and flow regime effects on C_d when the throat's strangulation isn't fully developed $Ma \approx 1$ in an experimental and numerical way.

RIVERA-LÓEPZ, Jesús Eduardo, ARCINIEGA-MARTÍNEZ, José Luis, LÓPEZ-AGUADO-MONTES, José Luis and GUTIERREZ-PAREDES, Guadalupe Juliana. Experimental and numerical calibration in a critical flow venturi of close to sonic flow. Journal of Engineering Applications. 2023

Operating principle of convergent-divergent sections

When a compressible flow flows through a convergent-divergent section, gas velocity reaches a maximum value in the minimum surface point (nozzle's throat), and the throat velocity fluid increases in function of an upstream and downstream pressure difference, this velocity limit value is the sound velocity or critical condition [5;19]. Under this condition, the Venturi nozzle is blocked or strangled, given that the block is a physical restriction caused by critical flow, the maximum mass flow rate that flows in the throat Venturi nozzle is given in this condition. In a dimensionless flow with negligible viscosity, theoretically, a relation can be used to predict critical Venturi nozzle metrological behavior, and, using this approximation, it can be demonstrated an ideal flow across a nozzle is governed by the following equation [17].

$$\dot{m}_{ideal} = \frac{P_0 A^* C^*}{\sqrt{R_{gas} T_0}} \tag{1}$$

This analytical model assumes that flow across the Venturi nozzle presents critical flow characteristics ($Ma = 1$). According to CODATA 2018, the universal gas constant is equal to $Ru = 8.314\ 462\ 618$ [J mol-1 K-1]. From Pitchard [1] molecular air mass is equal to 28,96546 kg/kmol.

If required a better estimation of mass rate, it's recommended to experimentally calibrate the Venturi nozzle, when the Venturi's discharge coefficient is a supplement of the ideal flow considerations, equation (1).

The discharge coefficient C_d [5] is defined as:

$$C_d = \frac{\dot{m}_{real}}{\dot{m}_{theorical}} \tag{2}$$

Aaron [2] defined the discharge coefficient as always less than unity, this condition assumes C_d calculation by using the real throat diameter, and the mass flow rate is not affected by vibrational relaxation. For a given Venturi nozzle geometry, the discharge coefficient variates as a function of flow relation through the same, and most frequently this function is expressed in Reynolds number terms defined by John D. Wright [21]:

$$Re = \frac{4\dot{m}_{real}}{\pi d \mu_0} \tag{3}$$

$$\mu_0 = \left(\frac{145,8\ T_0^{1,5}}{110,4 + T_0}\right) \tag{4}$$

Where: μ_0 – units are Pa·s and T_0 is Kelvin.

Calculation of the discharge coefficient "C_d"

The methodology provided by Standard ISO-9300, for mass flow rate calculation through a critical Venturi nozzle, includes the following restrictions:

-   Isentropic flow.

-   Dimensionless flow.

-   Perfectly calorific gas fluid.

Equations (1, 2 y 3) are completed with the restrictions presented before and the following expressions:

Critical flow coefficient C^* involves thermodynamic changes in the isentropic flow of the nozzle throat under stagnation conditions. In real gas applications, C^* depends on pressure, temperature, and chemical gas composition [21].

$$C^* = 0,68309 + 1,42025 X 10^{-5} T_0 - 2,80046 X 10^{-5} T_0 + 3,47447 X 10^{-5} P_0 - 1,80997 X 10^{-7} P_0 T_0 + 2,46278 X 10^{-10} P_0 \tag{5}$$

Where: P_0- is given in kPa, T_0 - in Kelvin.

If compressibility effects in the Venturi's throat want to be known, Mach dimensionless number must be used:

$$Ma = \frac{V}{c} \tag{6}$$

Where, environment's velocity V is determined by the mass flow rate, the throat diameter d, and the stagnation density ρ_0; stagnation density is determined by the state equation of perfect gasses.

$$V = \frac{4\dot{m}}{\pi d^2 \rho_0} \tag{7}$$

The sound velocity c in the throat is determined by the stagnation temperature T_0, thus:

$$c = \sqrt{\gamma R_{gas} T_0} \tag{8}$$

RIVERA-LÓEPZ, Jesús Eduardo, ARCINIEGA-MARTÍNEZ, José Luis, LÓPEZ-AGUADO-MONTES, José Luis and GUTIERREZ-PAREDES, Guadalupe Juliana. Experimental and numerical calibration in a critical flow venturi of close to sonic flow. Journal of Engineering Applications. 2023

Substituting equations 7 and 8 in 6, an expression to estimate the *Ma* number is obtained.

$$Ma = \frac{4\dot{m}\sqrt{T_0 R_{gas}}}{\pi d^2 P_0 \gamma^{1/2}} \qquad (9)$$

Flow is given in kg/s, *d* en meters, ρ_0 in kg/m³, γ is the specific heat relation, R_{gas} – is expressed in J/kg·K, T_0 – in Kelvin.

Specific heat relation, γ, can be determined by [21]:

$$C^* = 0,68309 + 1,42025X10^{-5}T_0 - 2,80046X10^{-5}T_0 + 3,47447X10^{-5}P_0 - 1,80997X10^{-7}P_0T_0 + 2,46278X10^{-10}P_0 \quad (10)$$

Where, P_0 is given in kPa and T_0 - in Kelvin. Finally, the discharge coefficient C_d [21], is estimated by the following equation:

$$C_d = \frac{4\dot{m}\sqrt{R_{gas}T_0}}{\pi d^2 C^* P_0} \qquad 11)$$

Experimental calibration and estimation of uncertainty

Venturi nozzles used in this work are from Flow System© with throat diameters of 0,088 in (2,24 mm) and 0,022 in (0,56 mm). The calibration patron used is based on a quantity of volume recollection in a lapse of time, the volumetric flow rate in charge of moving the piston or bell is calculated by the pulses and recollection time, the equation that allows to calculate the flow through the patrons is the following:

$$Q = \frac{C \cdot 60}{Kt} \qquad (12)$$

Where *K* is a constant equal to 543,2 pulses/L for the bell's patron and 13655,8 pulses/L for the piston, *C* is the number of pulses and t is the recollection time [16]. The mass flow rate will be estimated by multiplying equation twelve by the density of gas in the bell or piston. In air density measure floatability correction in wet air is currently the biggest part of uncertainty [1]. Besides, humidity in air causes deviation in the ideal behavior of thermodynamic properties of the fluid [9], thus, to use the equations presented before, calibration will be realized under the flow condition *HR* ≈ 0, therefore calculation of ρ, γ and *C, will be under dry air conditions, then equations 5, 10, and 13 are valid. Density is calculated by [21]:

$$\rho = \frac{1}{1,23838+287,04\frac{T_P}{P_P} - 30122 T_P^{-1,334}} + \frac{1}{-7,3049X10^{-4}\frac{P_P}{T_P}+2,5304X10^{-2}\frac{P_P}{T_P^{1,25}}} \qquad (13)$$

Where density is given in g/cm³, P_P units are kPa and T_P are Kelvin. From equations 12 and 13 mass flow rate is calculated, equation 14.

$$\dot{m} = \frac{C \cdot 60}{Kt}\rho \qquad (14)$$

To find uncertainty is suggested to use the law of propagation uncertainty [6;20], equation 15.

$$u_C^2 = \sum_{i=1}^{N} \left(\frac{\partial f}{\partial x_i}\right)^2 u_{x_i}^2 \qquad (15)$$

Where $f = f(x_1, x_2, x_3 \ldots \ldots \ldots \ldots x_n)$ then $u(f)$ is given by equation 15.

CENAM expressed their measures with a trust level not less than 95% (*p* = 95,45 %) [20], the purpose is to have a coverage factor *k* = 2,00 on normal distribution limit, therefore, all calculations realized in this work will have this coverage level. Calibration points between venturi nozzles are the pressures *P* of 200, 300, 400, 500 y 600 kPa, having a barometric pressure P_b = 80365 Pa. Tables 1 and 2 show average data measured of six realized repetitions for each calibration point for both critical flow Venturi nozzles.

P (kPa)	T (K)	P_p (kPa)	T_p (K)	C (pulses)	t(s)
200,83	294,21	80,78	293,93	60187,00	40,77
300,40	294,21	80,79	293,94	60313,50	27,14
400,67	294,18	80,81	293,96	60637,50	20,39
500,09	294,55	80,82	293,03	60739,67	16,33
601,25	294,59	80,83	293,02	60,741,83	13,62

Table 1 Experimental average data measured, d = 0,56 mm
Source: Own elaborated

P (kPa)	T (K)	P_p (kPa)	T_p (K)	C (pulses)	T (s)
200,48	293,04	80,91	293,17	60217,33	59,51
300,49	293,17	80,92	293,16	60386,33	39,58
400,46	293,29	80,93	293,16	60460,50	29,67
500,44	293,39	80,94	293,17	60607,67	23,85
600,83	293,36	80,95	293,20	60238,50	19,66

Table 2 Experimental average data measured, d = 2,24 mm
Source: Own elaborated

RIVERA-LÓEPZ, Jesús Eduardo, ARCINIEGA-MARTÍNEZ, José Luis, LÓPEZ-AGUADO-MONTES, José Luis and GUTIERREZ-PAREDES, Guadalupe Juliana. Experimental and numerical calibration in a critical flow venturi of close to sonic flow. Journal of Engineering Applications. 2023

Article

Using experimental data from Tables 1 and 2 as well as equations 12, 13 and 14, volumetric flow rate Q, density, ρ, and mass flow rate, $\dot{m}$, are going to be calculated.

With mass flow rate estimation and using stagnation enthalpy concept for an ideal gas and an isentropic stationary flow [19], stagnation pressure, P_0, and temperature, T_0, can be determined in the entrance of the Venturi:

$$T_0 = T_1 + \frac{\frac{1}{2}V_1^2}{c_p} \qquad (16)$$

The condition belongs to the Venturi entrance measures, P_0 y T_0. From continuity and state equation, the following equations are obtained:

$$V_1 = \frac{4\dot{m}}{\rho_1 \pi d_1^2} \qquad (17)$$

$$\rho_1 = \frac{P_1}{R_{gas}T_1} \qquad (18)$$

Substituting equations 17 and 18 in 16:

$$T_0 = T_1 + \frac{1}{2c_p}\left(\frac{4\dot{m}R_{gas}T_1}{\pi d^2 P_1}\right)^2 \qquad (19)$$

Mach number (air) in the Venturi entrance is calculated using the result of equation 19 [18]:

$$Ma = 5\left[\frac{T_0}{T_1} - 1\right] \qquad (20)$$

Stagnation pressure is determined by using equation 20 result:

$$P_0 = P_1[1 + 0,2Ma^2]^{3.5} \qquad (21)$$

Results of equations 19 and 21 are used to calculate critical flow factor C^* and discharge coefficient C_d, equations 5 and 11. Following the procedure described in section 3, uncertainty in measures is determined, in Tables 3 and 4.

$\dot{m}$ (kg/s)	P_o (kPa)	T_0 (K)	C^*	C_d	u_{Cd} (%)
0,00010	201,32	294,41	0,6878	0,8881	0,026
0,00016	301,29	294,46	0,6881	0,8934	0,021
0,00021	402,00	294,46	0,6884	0,8964	0,020
0,00026	501,89	294,85	0,6887	0,8984	0,019
0,00031	603,01	294,90	0,6889	0,8954	0,020

Table 3 Calibration results, d= 0,56 mm
Source: Own elaborated

$\dot{m}$ (kg/s)	P_o (kPa)	T_0 (K)	C^*	C_d	u_{Cd} (%)
0,00179	201,05	293,28	0,6878	0,9605	0,031
0,00270	301,54	293,46	0,6881	0,9662	0,027
0,00361	402,02	293,61	0,6884	0,9682	0,026
0,00450	502,53	293,74	0,6887	0,9663	0,028
0,00543	603,48	293,73	0,6889	0,9696	0,030

Table 4 Calibration results, d = 2,24 mm
Source: own elaborated

By Reynolds (Re) and Mach (Ma) dimensionless numbers, calibration results are graphed, to calculate these dimensionless numbers, equations 3, 4, 9, and 10 are used. The results are shown in Tables 5 and 6.

μ_0 (Pa·s)	γ	Re	Ma
0,000127	1,42	1853,06	0,890
0,000127	1,42	2789,69	0,895
0,000127	1,42	3735,07	0,898
0,000127	1,42	4666,57	0,901
0,000127	1,42	5596,66	0,899

Table 5 Calculation of μ_0, ɣ, Re y Ma, Venturi nozzle d = 0,56 mm
Source: own elaborated.

μ_0 (Pa·s)	γ	Re	Ma
0,000127	1,40	8042,42	0,962
0,000127	1,41	12124,95	0,968
0,000127	1,41	16190,18	0,970
0,000127	1,41	20190,60	0,968
0,000127	1,41	24338,66	0,972

Table 6 Calculation of μ_0, ɣ, Re y Ma, Venturi nozzle d = 2,24 mm
Source: own elaborated

Analysis of results

According to the results obtained, discharge coefficients for both Venturi nozzles increase in function of flow regime, Figure 1, uncertainty associated in each calibration point is shown in Tables 3 and 4, from this, estimated uncertainty in the stabled limits by [10]. Comparing obtained results with Chunhui's shown uncertainty estimation is close to values reported by [4], which proves good measure practice and accurate procedure of uncertainty estimation developed in this calibration.

Aaron [2] reported CFV calibration in laminar, transition, and turbulent flow, 7.2 X 10^4 ≤ Re ≤ 2.5 X 10^6, from this it can be determined for both Venturi nozzles calibration was realized in laminar and turbulent flow, see Graphs 1 and 2.

RIVERA-LÓEPZ, Jesús Eduardo, ARCINIEGA-MARTÍNEZ, José Luis, LÓPEZ-AGUADO-MONTES, José Luis and GUTIERREZ-PAREDES, Guadalupe Juliana. Experimental and numerical calibration in a critical flow venturi of close to sonic flow. Journal of Engineering Applications. 2023

Dispersion in Graph 2 shows the linear data adjust, the adjusted result are empirical equations 22 and 23 for Venturi nozzles of 0,56 and 2,24 mm respectively, which will be discussed later.
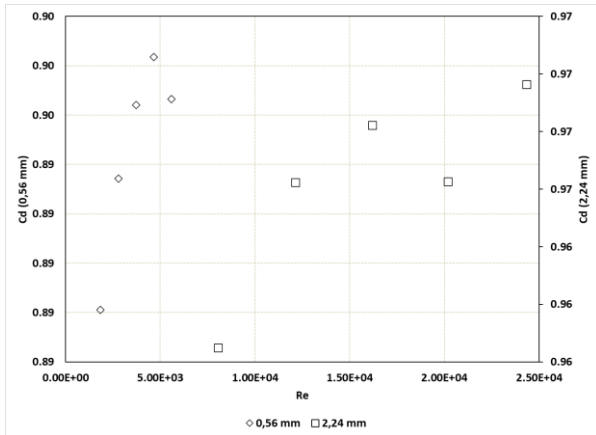
Graphic 1 Calibration results, C_d vs Re, 0,56 y 2,24 mm
Source: Own elaborated

In both Venturi nozzles, the Flow regime is totally viscous, and this way, the relation $1/Re^{0,5}$ increases because the flow regime decreases, and C_d decreases linearly. The prevalence of viscous forces produces the deviation of real flow in respect of theoretical value from equation one, as said by Cruz-Maya [8], for this reason, high viscous shear stress in the boundary layer leads to a maximum area on the throat having as result that the throat's flow won't be the maximum as theory indicates for adiabatic-isentropic flow in divergent-convergent sections [5;19] and, therefore, it will directly and irreversibly affect the C_d magnitude from the ideal value. In addition, C_d magnitude also depends on flow compressibility, Ma; the effective area in the throat when sonic flow is achieved Ma=1, under this flow condition, small variations of static pressure through the transversal plane in the throat won't have any important effect on mass flow rate $\partial\rho\forall/\partial P$ [18], therefore, mass flow rate will be constant because static pressure keeps boundary layer thickness reduced to its minimum value, $\delta(x)_{min}$. In the boundary layer thickness $\delta(x)$ flow is supersonic $Ma > 1$ and outside the boundary layer the flow is subsonic $Ma < 1$[8]. In figure 3 subsonic flow is shown, the 0,56 mm Venturi nozzle is further from sonic condition and therefore its C_d is lower while 2,24 mm Venturi nozzle diameter has a higher C_d because the throat flow is almost sonic condition, Ma was estimated in the throat's center.

Best calibration points for both Venturi nozzles occur under low relation values $1/Re^{0,5}$, which means, regimen flow is about to stop being viscous, and is close to sonic condition, for example, for d = 2,24 mm its best calibration point is C_d = 0,9696 for a regime Re = 24338,66 and Ma = 0,972, see tables 4 and 6. However, for d = 0,56 mm nozzle every calibration point in the flow are in a total viscous and subsonic regime, so the discharge coefficient has dissipative, dynamics and hydrostatic unwished effects, since the maximum value is C_d = 0,8984 with Re = 4666,57 and Ma = 0,899, see tables 3 and 4.
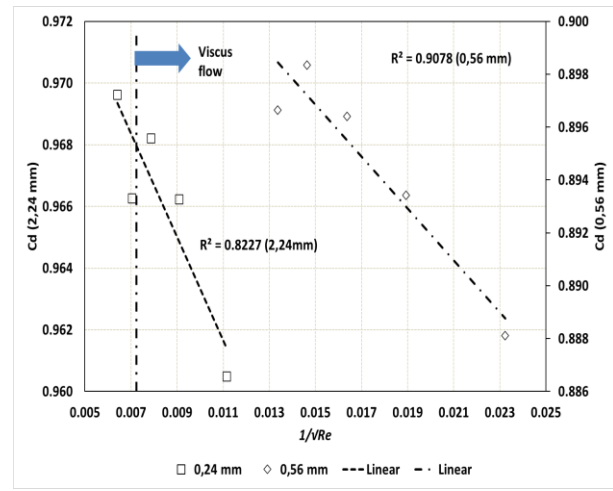
Graphic 2 C_d vs $1 / Re^{0,5}$
Source: Own elaborated

$$C_d = 0,9116 - \frac{0,9819}{\sqrt{Re}} \qquad (22)$$

$$C_d = 0,9801 - \frac{1,6807}{\sqrt{Re}} \qquad (23)$$
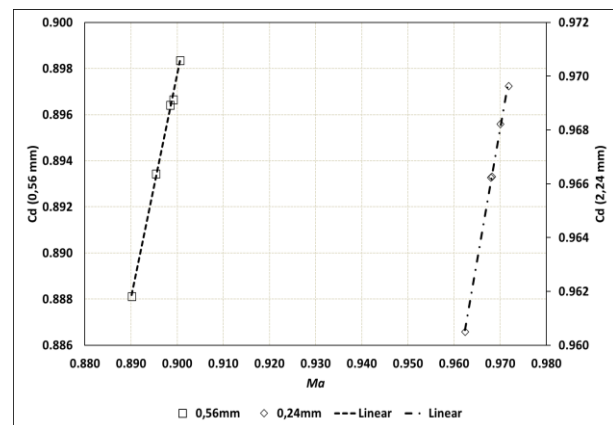
Graphic 3 Compressible Flow in the throat, C_d vs Ma
Source: Own elaborated

RIVERA-LÓEPZ, Jesús Eduardo, ARCINIEGA-MARTÍNEZ, José Luis, LÓPEZ-AGUADO-MONTES, José Luis and GUTIERREZ-PAREDES, Guadalupe Juliana. Experimental and numerical calibration in a critical flow venturi of close to sonic flow. Journal of Engineering Applications. 2023

From the shown data, it is important to understand the totally viscous compressible flow mechanism about the realized calibration and above all to understand how this flow regimen affects the discharge coefficient magnitude, thus, by using computational fluid dynamics (CFD) an experiment in totally viscous regimen is realized, the software ANSYS® 2020 R1 student's version is used.
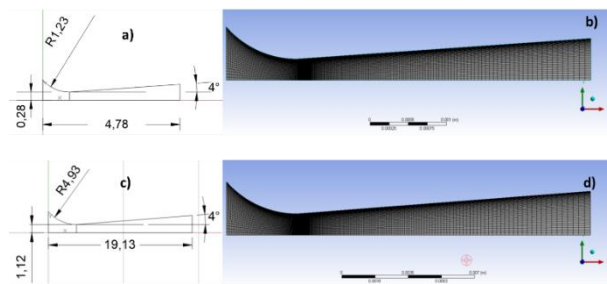
Figure 1 Venturi nozzle geometries and computational space discretization
Source: own elaborated

Figures 1a y 1c, show the principal dimensions for d = 0,56 mm and d = 2,24 m Venturi nozzles, respectively. Figures 1b and 1d show discretization of the computational space with structured meshing, where d = 0,56 mm Venturi has a density of 10459 elements and d = 2,24 mm has a density of 10234 elements, it also shows the logarithmic increase of the mesh for the wall and the throat zone to obtain a good estimation of the throat velocity profiles. The numerical experimental conditions are: symmetric-axis, stationary, ideal gas (air), turbulence model k-ε realizable, solver density-base. The experiment got solved for Pressure-inlet-Pressure-outlet conditions, where boundary conditions for the entrance are total pressure P_0 and entrance temperature T_0, showed in tables 3 and 4. According to results discussed on Graph 3, global flow in the throat is Ma <1, this is the reason why in the Venturi exit plane the only back pressure will be atmospheric pressure, thus, to determinate the exit boundary condition is needed the Venturi nozzles geometries, knowing them, the area between the throat and the exit plane is determined, A_e/A^*, using this result and the interpolation of isentropic relations for an ideal gas (Υ = 1.4), Ma_e and P_e/P_0 can be known in the exit plane of the Venturi nozzles, see Table 7.

Diameter	A_e/A^*	P_e/P_0	Ma_e
0,56 mm	1.96	0,098	2,17
2,24mm	2.1	0,087	2,25

Table 7 Isentropic relations in the exit plane
Source: Own elaborated

The obtained results from the numerical experiment are shown in Graph 4. The figure shows the velocity profiles of Blassius u/U, as a function of r/d for each diameter throat and each stagnation pressure. The standard velocity profile has a cero value on the wall, so the separation gets the boundary layer thickness $r = \delta(x)$, the standard velocity profile reaches its maximum value u/U = 0,99 in supersonic regime Ma > 1. The flow acceleration in the boundary layer is caused by the viscous dissipation, since the friction between the flow and the wall increases the flow internal energy, and by consequence, the temperature increase will cause a decrease the flow density, the flow must accelerate in the small displacement thickness δ^*. Outside the viscous zone flow is subsonic, and the relation u/U will be more sensible to the pressure gradients change dP/dr, see Graph 4 and 5. From Graph 5, outside the boundary layer, gradient is unfavorable, dP/dr > 0, flow is adverse and the profile u/U decreases against the flow direction. In the wall region the gradient is favorable, dP/dr < 0, the profile u/U increases in the flow direction and reaches its maximum value in viscous zone limit.
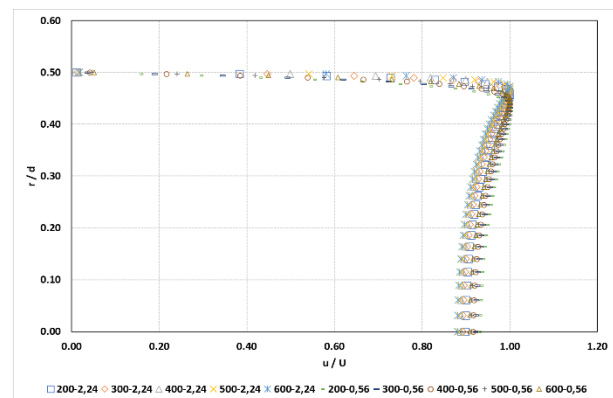
Graphic 4 Standard velocity profiles, 0,56 y 2,24 mm
Source: Own elaborated
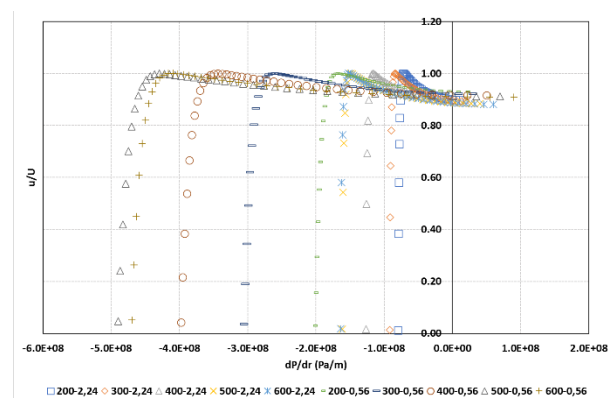
Graphic 5 Profile u/U vs dP/dr, 0,56 y 2,24 mm
Source: Own elaborated

RIVERA-LÓEPZ, Jesús Eduardo, ARCINIEGA-MARTÍNEZ, José Luis, LÓPEZ-AGUADO-MONTES, José Luis and GUTIERREZ-PAREDES, Guadalupe Juliana. Experimental and numerical calibration in a critical flow venturi of close to sonic flow. Journal of Engineering Applications. 2023

The standard velocity profile is used to find the displacement thickness $\delta*/d$ in the throat, thus, pressure gradient in the wall is considered as zero, $dP/dx = 0$ [18; 19] and the velocity profile behavior will be approximate to a laminar and parabolic behavior in the boundary layer thickness. To sustain the laminar and parabolic velocity profile consideration, the shape factor H was calculated, thus, Jea-Hyung equations are used [11] to calculate the displacement thickness $\delta*$ and the moment thickness θ, the results are shown in Graph 6. In the Figure is appreciated factor H depends on the throat diameter, the stagnation pressure, and the pressure gradient in the wall zone. Outside the viscous region, H is independent of r/d, therefore, H approximates to a constant and will only be lightly modified by the pressure gradient. The red and blue color ovals in the figure indicate the immediate zone on the wall where viscous effects predominate, as value $H > 2,0$ indicates, and particularly in the throat diameter of 0,56 mm this effect is remarkable since despite stagnation pressure increases and by consequence velocity increases as well, the H difference is 0,24 % in the test interval. In both throat diameters flow is totally laminar on the wall zone, as reported [18], therefore a parabolic and laminar profile approximation can be used in the boundary layer thickness.
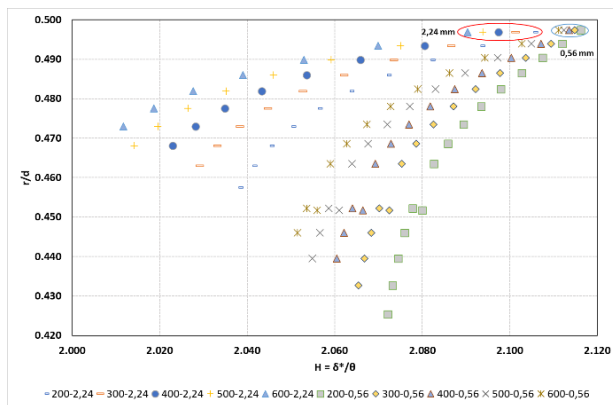
Graphic 6 Shape factor H, 0,56 y 2,24 mm
Source: Own elaborated

The literature stablished [5;20] the boundary layer thickness δ has its maximum value when $u/U = 0,99$, using this consideration, in Graph 4 results, dispersion data from the wall to the maximum value $\delta(x)$ are extracted, see Graphs 7 and 8. The figures show the standard profiles in the boundary layer thickness δ for the throat diameters, it also shows the data adjust and the adjust quality factor which indicates the good adjust quality, since $R^2 \approx 1$, figure presents too the adjust equations obtained.
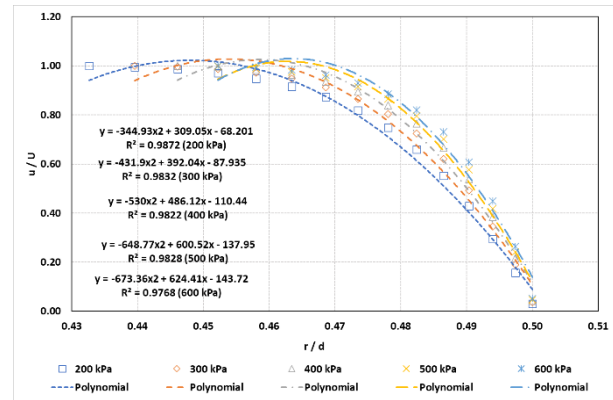
Graphic 7 Standard profiles in viscous zone, 0,56 mm
Source: Own elaborated
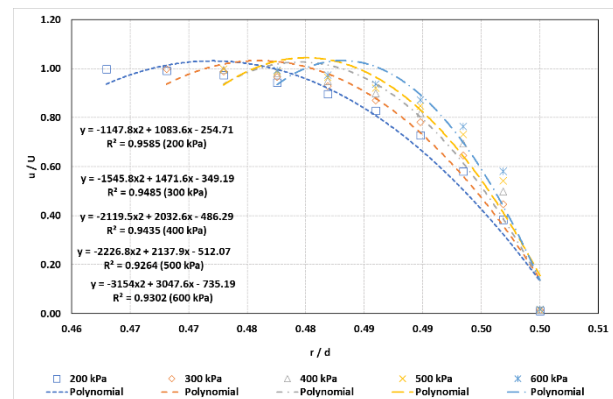
Graphic 8 Standard profiles in viscous zone, 2,24 mm
Source: Own elaborated

Substituting velocity profiles equations in the momentum integral equation for a zero-pressure gradient, the thickness movement $\delta*$ in function of Re and the flat-plate's longitude x. To obtain the equation as function of the throat diameter the Stratford equation [18] for equivalent length must be used. In Graph 9 shows obtained results, the $\delta*/d$ behavior is linear from the region near the wall to the boundary layer thickness, the ovals in the graphic point out the maximum value of the relation $\delta*/d$ which belongs to the thickness movement for each throat diameter and stagnation pressure. The viscous regime is superior in the Venturi nozzle of 0,56 mm diameter hence it has the higher values of $\delta*/d$, and because the flow velocity is higher in the throat diameter of 2,24 mm the viscous effects affect in less proportion the thickness movement, since it has lower values of relation $\delta*/d$ than the other diameter under the same stagnation conditions. From the movement thickness data, the lineal adjust is realized as shown is Graph 9, in the figure is also seen the good quality of the adjust, since $R^2 \approx 1$, the equations 24 is the lineal variation of the relation $\delta*/d$ as function of the flow regime.

RIVERA-LÓEPZ, Jesús Eduardo, ARCINIEGA-MARTÍNEZ, José Luis, LÓPEZ-AGUADO-MONTES, José Luis and GUTIERREZ-PAREDES, Guadalupe Juliana. Experimental and numerical calibration in a critical flow venturi of close to sonic flow. Journal of Engineering Applications. 2023
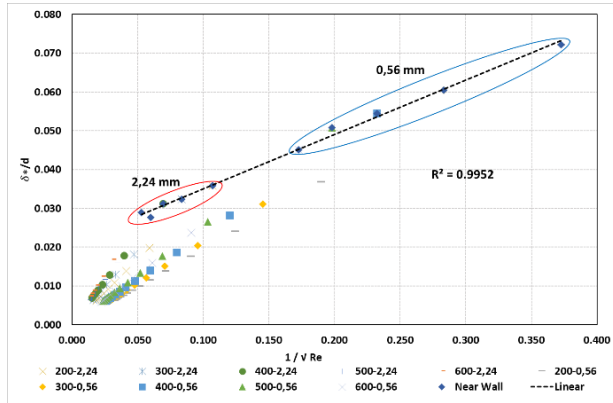
Graphic 9 Movement thickness as function of $Re^{-0,5}$
Source: Own elaborated

$$\frac{\delta^*}{d} = 0,021 + \frac{0,1401}{\sqrt{Re}} \qquad (24)$$

Earlier was discussed the importance of flow compressibility in the throat nozzle, see Graph 3, in that sense, the δ^*/d relation is shown in Graph 10 as a function of Ma number. In the graph is shown the variation of the relation δ^*/d as function of Ma from the movement thickness to the boundary layer thickness. In the thickness of movement (ovals) is appreciated that compressibility reduces the thickness δ^*/d dimension and thence improves the throat strangulation; the 2,24 mm throat has a value of 35,92% smaller than 0,56 mm in equal conditions of stagnation, 600 kPa, which provokes a better estimation of C_d for this throat diameter. Using the data in the thickness of movement an adjust is realized, in the graph is shown the good quality of the adjust, since $R^2 \approx 1$.

$$\frac{\delta^*}{d} = 0,0196 Ma^{-0,64} \qquad (25)$$

Equation 25 is the potential variation of the relation δ^*/d as a function of Mach number, this proposition's objective is to estimate the size and behavior of the thickness of movement by the flow compressibility, this equation is proposed to be used for the interval $0,14 \leq Ma \leq 0,6$, and presents the necessity of realized another studies to validate this empirical model.
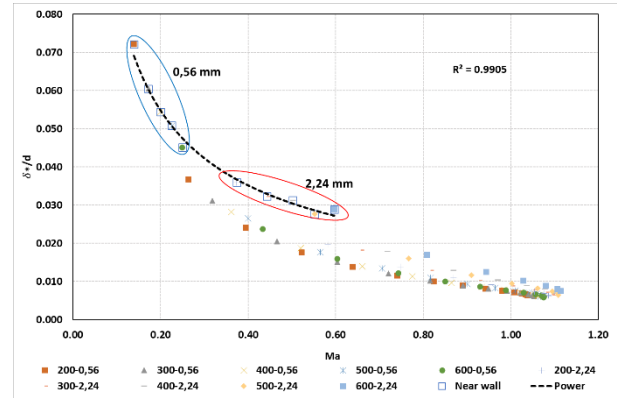
Graphic 10 Thickness movement in function of Ma
Source: Own elaborated

Given that viscosity and compressibility effects affection on the thickness of movement size were widely discussed, now is proceeded to the estimation of the discharge coefficient, Stratford [18] reported that the discharge coefficient in the viscous region is $(1 - C_{dvis}) = 4\delta^*/d$, with the thickness of movement results, the C_{dvis} in the viscous is estimated, the equation 26 represents the C_{dvis} variation for throat diameters of 0,56 and 2,24 mm.

$$C_{dvis} = \frac{0,5604}{\sqrt{Re}} \qquad (26)$$

Now the discharge coefficient in the free stream zone is determined, C_{d-inv}, Cruz Maya [8] developed an integral equation for momentum along the sonic line for stationary, compressible, dimensionless, and uniform properties flow, see equation 27, where ρ is the density, a is the sound's velocity in the throat, γ is the specific heat relation under stagnation conditions and P is the static pressure in the throat.

$$C_{dinv} = \left(\frac{\rho a^2}{\gamma_0 P}\right)_{th} \qquad (27)$$

From results of the numerical experiment C_{dinv} is calculated as function of radial position, as Cruz-Maya said the term $(\rho\, a^2/\, P)$ takes different values in the radial plane of the nozzle throat, combining rests between the limits of 0 and 1, and for each stagnation pressure and throat diameter the results are $0,9945$ and $0,9261$ for 2,24 y 0,56 mm respectively. The total discharge coefficient is $C_d = 1- (Cd_{vis}-1) - (Cd_{inv}-1)$ [8,18], therefore the coefficients end as following:

$$C_d = 0,9882 - \frac{0,5604}{\sqrt{Re}} \qquad (28)$$

$$C_d = 0,9261 - \frac{0,5604}{\sqrt{Re}} \qquad (29)$$

RIVERA-LÓEPZ, Jesús Eduardo, ARCINIEGA-MARTÍNEZ, José Luis, LÓPEZ-AGUADO-MONTES, José Luis and GUTIERREZ-PAREDES, Guadalupe Juliana. Experimental and numerical calibration in a critical flow venturi of close to sonic flow. Journal of Engineering Applications. 2023

Equations 28 and 29 are the numerical coefficients in flow close to the throat's strangulation for diameter of 2,24 and 0,56 mm respectively, these two models are now compared to experimental results, empirical equations 22 and 23, as well as ISO 93000 [17] and Ishibashi's [7] equation, see graph 11.
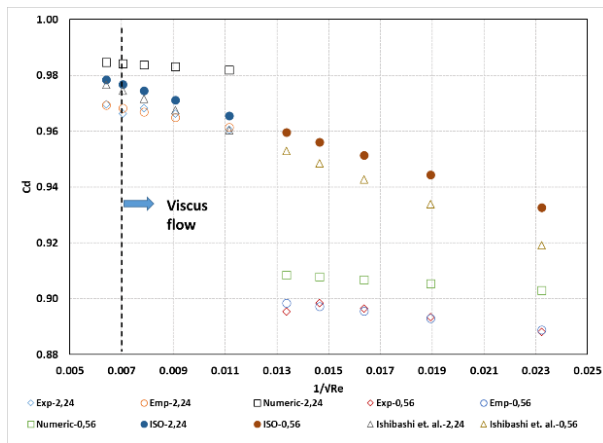
Graphic 11 Numerical, experimental and empirical discharge coefficient for 2,24 and 0,56 mm diameters and comparative
Source: Own elaborated

The discharge coefficients from Figure 12 show in flow regime close to turbulent $1 / Re^{0.5} \approx 0,007$ the ISO 9300 and Ishibashi models are close to experimental C_d.

Of 2,24 mm since the maximum error is from 1,07 to 0,84% respectively, however for the numerical model, equation 28, the maximum error is 2,18% for totally viscous zone, the empirical model in equation has a maximum error of 0,2%, it's important to indicate the numerical model's estimation improves as the flow regime approximates to turbulent region, since the minimum error is 1,52%.

With respect to C_d results for 0,56 mm the models of ISO 9300 and Ishibashi have errors of 6,68 and 6,03%, respectively, therefore they're not a good choice for calibration in totally viscous region, in respect of the numerical model it shows an acceptable performance, since the maximum error is 1,64 % and improves the estimation in a way the flow regime increases, finally empirical equation 22, has a maximum error of 0,32 %, meaning it is the best calibration option in totally viscous regime.

Conclusions

Likewise, it can be concluded that:

1. The calibration in $Ma \approx 1$ flow causes dissipative, dynamics and hydrostatic unwished effects on the thickness of movement δ^*, therefore in the C_{dvis} magnitude, and these effects are prevalent for the 0,56 mm throat's diameter since relation δ^*/d is 35,92% bigger than 2,24 mm throat's diameter.

2. Numerical models are a bad estimation of C_d under these stagnation conditions since the maximum error estimated is 6,68% and is superior in the 0,56 mm throat's diameter.

3. The empirical models are a good estimation of C_d since the errors for both Venturi nozzles weren't higher than 1% and for these flow conditions the best option is experimental calibration.

4. 2,24 mm throat diameter can reach better results if the flow regime keeps increasing to get close to sonic condition and therefore avoid static pressure variation affection on the C_d magnitude.

5. The measure uncertainty was satisfactory estimated, therefore good quality on obtained results in this work are assured.

Nomenclature

A	*Surface*
CFV	*Critical Flow Venturi*
c	*Number of pulses*
C^*	*Johnson's critical flow factor*
C_d	*Discharge coefficient of the nozzle*
C_{d-vis}	*Viscous discharge coefficient*
$C_{d-invis}$	*Inviscous discharge coeffient*
d	*Venturi nozzle throat diameter*
δ	*Boundary layer thickness*
δ^*	*Thickness of movement*
K	*National's patron calibration constant*
k	*Coverage factor*
γ	*Specific heats relation*
m_{ideal}	*Ideal mass flow rate*
m_{actual}	*Actual mass flow rate*
Ma	*Mach number*
N	*Contributions number*
Pp	*Pressure patron*
P_0	*Stagnation pressure*
p	*Trust level*
Q	*Volumetric flow rate*
$Rgas$	*Gasses constant*

RIVERA-LÓEPZ, Jesús Eduardo, ARCINIEGA-MARTÍNEZ, José Luis, LÓPEZ-AGUADO-MONTES, José Luis and GUTIERREZ-PAREDES, Guadalupe Juliana. Experimental and numerical calibration in a critical flow venturi of close to sonic flow. Journal of Engineering Applications. 2023

Re	*Reynolds number*
T_P	*Patron temperature*
To	*Stagnation temperature*
u_{cd}	*Discharge coefficient uncertainty*
ρ	*Patron's air density*
μ_0	*Viscosity under stagnation conditions*
t	*Recollection time of gass*

Superscripts

o	*Stagnation conditions*
*	*Critical conditions*

Subscripts

e	*Output conditions*

Acknowledgement

Funding

References

[1] A Picard, R. S. (2008). Revised Formula for the Density of Moist Air. *Metrología 45*, 149-155. doi:10.1088/0026-1394/45/2/004

[2] Aaron Johnson, J. W. (2008). Comparison Between Theoretical CFV Flow Models and NIST's Primary Flow Data in the Laminar, Turbulent and Transition Flow Regimes. *Journal of Fluids Engineering ASME.* http://fluidsengineering.asmedigitalcollection.asme.org/pdfaccess.ashx?url=/data/journals/jfega4/27324/ on 07/08/2017

[3] B. Mikan, R. K. (2006). Determination of discharge coefficient of critical nozzles based on their geometry and the theory of laminar and turbulent boundary layers. *Proceedings of the 6th International Symposium on Fluid Flow Measurement.*

[4] Chunhui Lia, P. a. (2018). Throat Diameter Influence on the Flow Characteristics of Critical Venturi Nozzle. *Flow Measurement and Intrumentation* , 105-109. https://doi.org/10.1016/j.flowmeasinst.2018.02.012

[5] Fox, R. W. (2011). *Introduction to Fluid Mechanics.* USA: Wiley and Sons Inc.

[6] (2002). *Guía para la expresión de la incertidumbre en las mediciones.* Norma Mexicana NMX-CH-140-IMNC-2002.

[7] Ishibashi, M. (2015). Discharge Coefficient equation for critical-flow toroidal-throat venturi nozzles covering the boundary-layer transition regime. *Flow Measurement and Instrumentation*, 107-121. http://dx.doi.org/10.1016/j.flowmeasinst.2014.11.009

[8] J. A. Cruz-Maya, F. S. (2006). A new correlation to determine the discharge coefficient of a critical Venturi nozzle with turbulent boundary layer. *Flow Measurement and Instrumentation*, 258-266. doi:10.1016/j.flowmeasinst.2006.06.002

[9] J. M. Lim, B. H.-A. (2011). The humidity effect on air flow rates in a critical flow venturi nozzle. *Flow Measurement and Intrumentation*, 402-405. doi:10.1016/j.flowmeasinst.2011.06.004

[10] J.A., C. M. (2005). Analytical and Numerical Characterization of the Discharge Coefficient of a Sonic Venturi Nozzle. *Ph. D. Thesis Instituto Politécnico Nacional.*

[11] Jae Hyung Kim, H. D. (2010). The Effect of Diffuser Angle on the Discharge Coefficient of a Miniature Critical Nozzle. *Journal of Thermal Science*, 222-227. DOI: 10.1007/s11630-010-0222-2

[12] John D. Wright, W. K. (2021). Thermal boundary layers in critical flow Ventures . *Flow Measurement and Instrumentation*, 102525. https://doi.org/10.1016/j.flowmeasinst.2021.102025

RIVERA-LÓEPZ, Jesús Eduardo, ARCINIEGA-MARTÍNEZ, José Luis, LÓPEZ-AGUADO-MONTES, José Luis and GUTIERREZ-PAREDES, Guadalupe Juliana. Experimental and numerical calibration in a critical flow venturi of close to sonic flow. Journal of Engineering Applications. 2023

[13] Junji Nagao, S. M. (2013). Characterictics of high Reynolds number flow in a critical nozzle. *International Journal of Hydrogen Energy*, 1-9. http://dx.doi.org/10.1016/j.ijhydene.2013.04.158

[14] Lambert Marc Antoine, R. M. (2021). Experimental Investigations on Cylindrical Critical Flow Venturi Nozzles with Roughness. *Flow Measurement and Instrumentation*, 102002. https://doi.org/10.1016/j.flowmeasinst.2021.102002

[15] Masahiro Ishibashi, M. T. (2000). Theoretical discharge coefficient of a critical circular-arc nozzle with laminar boundary layer and its verification by measurements using super-accurate nozzles. *Flow Measurement and Intruments* , 305-313.

[16] Rivera, J. E. (2006). *Diseño, construcción y caracterización de un banco de toberas sónicas para un laboratorio secundario de medición de flujo de gases.* Mexico.

[17] (1990). *Standard ISO 9300 Critical Measurement of Gass flow by Means of Flow Venturi Nozzles* .

[18] Stratford, B. S. (n.d.). The calculation of the discharge coefficient of profiled choked nozzles and the optimum profile for absolute air flow measurement . *Formely National Gas Turbine Establishment, Pystoch, now Rolls-Royce Ltd.* https://doi.org/10.1017/S0001924000060905

[19] White, F. (2009). *Fluid Mechanics* . USA: McGraw-Hill.

[20] Wolfgan A. Schmid, R. J. (2004). *Guía para la estimación de la incertidumbre* . CENAM.

[21] Wright, J. (1998). The Long Term Calibration Stability of Critical Flow Nozzles and Laminar Flowmeters . *Proceedings of the 1998 NCSL Workshop and Symposium (Standard ISO 9300 Critical Measurement of Glass flow by Means of Flow Venturi Nozzles, 1990)*, 443-462.